Soils and Rocks

An International Journal of Geotechnical and Geoenvironmental Engineering

www.soilsandrocks.com

ISSN 1980-9743
ISSN-e 2675-5475

Sustainable stabilization of clay soil with fly ash, GGBS, and sulfate resistance

Lakshmi Kant[1#], Sanjeet Kumar[1], Md Asfaque Ansari[1], Sunny Raj[1]

Article

Keywords
Sulphate resistance
Clay soil
Fly ash
Granulated blast furnace slag
Sustainable pavement base

Abstract

This study evaluates the use of Class F fly ash (FA) and ground granulated blast furnace slag (GGBS), traditionally considered a waste material, as a replacement and partially reactive material in geopolymer stabilization of lean clay (CL) soil for sustainable pavement applications. The effects of NaOH concentration (4M, 8M, 12M, and 16M), GGBS content (0%, 5%, 10%, and 15%), and curing duration (7, 28, and 60 days) on mechanical and durability properties were analyzed. Results showed that the 10% GGBS blend achieved the highest UCS of 13.62 MPa at 12M NaOH after 60 days, meeting Indian Roads Congress standards. Sulphate resistance tests revealed minimal UCS loss (2.83% at 4M) for the 10% GGBS mix, compared to 34.62% for blends without GGBS. Strength transitioned from ductile failure at 7 days to brittle failure at 60 days, indicating matrix development. A strong linear correlation (R^2 = 0.98) between UCS and stiffness (G) enables practical predictions. This research highlights the viability of FA-GGBS geopolymer blends as a sustainable alternative for soil stabilization in pavement applications, promoting resource utilization and waste reduction.

1. Introduction

Soil in its natural form is often unsuitable for large construction projects due to its low mechanical strength. For example, expansive soil alone accounts for 25% of structural failures in the USA (Jones & Jefferson 2023; Scheuermann Filho et al., 2022; Zinchenko et al., 2022) due to its tendency to shrink and swell with moisture changes. To address these limitations, soil treatment is necessary to enhance its physical and chemical properties suitability for construction applications. In developing countries like India, where rapid urbanization and population growth drive an increasing demand for infrastructure (Humbal et al., 2023; Ansari et al., 2024; Wang et al., 2024a; Bezerra et al., 2025), large-scale soil treatment is essential.

Soil stabilization is a multidisciplinary geotechnical procedure that involves mechanical, chemical, or other treatment techniques to enhance the chemical, physical, and mechanical properties of soil. This process plays a crucial role in achieving engineering objectives and is particularly essential for constructing roads, building foundations, and other infrastructure projects (Porbaha, 1998; Sharma et al., 2018; Suresh & Murugaiyan, 2021; Amiri et al., 2022). Traditionally, lime, cements and fly ash are used as chemical additives in chemical stabilizations of soil (Andavan & Pagadala, 2020; Consoli et al., 2021; Raja et al., 2022).

Currently, Ordinary Portland Cement (OPC) is widely used as cementing material for structural infrastructures including soil stabilization; however, its production generates significant amounts of CO_2. Globally, OPC production is responsible for approximately 4 billion tons of CO_2 emissions annually (Davidovits, 1994; Yusuf et al., 2014; Part et al., 2015), with India accounting for 7% of total cement consumption (Sahoo et al., 2023). This extensive use contributes substantially to greenhouse gas emissions and exacerbates the greenhouse effect. It was reported that nearly 1 ton of co2 emitted while producing 1 ton of OPC (Davidovits, 2013).

The rise in pollution, global warming, and public environmental awareness has driven the demand for eco-friendly construction materials, especially in developed and developing countries (Part et al., 2015; Mistri et al., 2020; Ahmad et al., 2021). Geopolymer, an innovative green cement made from industrial by-products, is emerging as a sustainable alternative to OPC (Shehata et al., 2022). It is an inorganic aluminosilicate material synthesized by combining silica (SiO_2) and alumina (Al_2O_3)-rich sources such as fly ash,metakaolin,ground granulated blast slag (GGBS), and silica fumewith alkali activators (Silva et al., 2007; Nagajothi & Elavenil, 2021; Zhang et al., 2021; Riyap et al., 2022; Sepehrian et al., 2024).

[#]Corresponding author. E-mail address: lakshmi.kantdst@bihar.gov.in
[1]Rashtrakavi Ramdhari Singh Dinkar College of Engineering Begusarai, Department of Civil Engineering, Begusarai, Bihar, India.

Submitted on December 11, 2025; Final Acceptance on May 23, 2026; Discussion open until November 30, 2026.

Editor: Renato P. Cunha

https://doi.org/10.28927/SR.2026.019725

Geopolymers exhibit a variety of engineering properties desirable for civil engineering applications. These include high compressive strength (Duxson et al., 2007; Amnadnua et al., 2013; Bagheri & Nazari, 2014), fast and controllable setting timing (Lee & Van Deventer, 2002; Ranjbar et al., 2020), excellent fire resistance (Sakkas et al., 2014; Sarker et al., 2014), and superior resistance to acid and salt solutions (Palomo et al., 1999; Vafaei et al., 2021). Furthermore, geopolymers are characterized by the absence of deleterious alkali-aggregate reactions and exhibit low shrinkage behavior (Zhang et al., 2013, 2022).

The most common activators in geopolymerization are sodium silicate and sodium hydroxide, known for enhancing mechanical properties but with notable environmental impacts (Handayani et al., 2022; Nanda et al., 2024). Sustainable alternatives, such as rice husk ash (RHA) processed with NaOH, offer comparable performance (Panitsa et al., 2024), while waste-derived activators like calcium carbide residue and coal gangue also show potential for improving geopolymer properties (Yan et al., 2023; Wang et al., 2024b).

Fly ash (FA), particularly types C and F, plays a key role in sustainable construction by replacing traditional cement, reducing carbon emissions, and utilizing industrial waste (Palomo et al., 2007; Temuujin et al., 2009; Hoy et al., 2017). Type C FA, rich in calcium oxide, exhibits self-cementing properties, achieving compressive strengths up to 70.80 MPa under optimal conditions and forming calcium silicate hydrate (CSH) and calcium alumino hydrate (CAH) with alkaline activators (Misra et al., 2005; Roskos et al., 2011; Astuti, 2024; Nurlina et al., 2024). Type F FA, requiring activators, enhances water permeability due to larger pore sizes and benefits from the inclusion of granulated blast furnace slag (GBFS), which forms aluminum-modified calcium silicate hydrate (CASH) and sodium aluminosilicate hydrate (NASH) gels, improving mechanical properties (Puertas et al., 2000; Kumar et al., 2010; Bernal et al., 2013; Ismail et al., 2014; Nurlina et al., 2024). The coexistence of CASH and NASH has also been observed in other FA and calcium-rich additive-based geopolymers, further enhancing material performance (Guo et al., 2010; Somna et al., 2011). The global production of over 250 million tons of fly ash annually emphasizes the need for sustainable use in geopolymers, which can lower carbon footprints and promote a circular economy (Abu Bakar et al., 2024; Gajghate & Nardey, 2024; Lin et al., 2024). However, challenges remain, such as variability in properties and environmental risks, requiring further research for optimization (Gajghate & Nardey, 2024).

Recent studies have expanded the use of geopolymers in stabilizing soft soils and demolition waste. For example, Phummiphan et al. (2017) used high-calcium fly ash-based geopolymers to stabilize marginal lateritic soil for green pavements in Thailand, enhanced by waste calcium carbide residue (CCR), which reacts with silica and alumina to form Calcium Silicate Hydrate (CSH) (Kampala & Horpibulsuk, 2013; Phummiphan et al., 2016). Phetchuay et al. (2016) applied fly ash-based geopolymers to stabilize soft marine clay in Australia, demonstrating CCR's ability to improve strength and provide a low-carbon alternative to cement stabilization. Geopolymers, activated with alkaline solutions, significantly improve soil shear strength—up to six times greater—and achieve unconfined compressive strength (UCS) values up to 1290 kPa within 14 days, depending on the molarity of the activating solution (Al Khafaji et al., 2024). Despite these benefits, challenges such as material variability and the need for further research on long-term performance remain (Arulrajah et al., 2016; Mohammadinia et al., 2016).

Fine-sized granulated blast furnace slag (GBFS) enhances the engineering properties of Class F fly ash (FA) in geopolymers, improving mechanical strength, durability, and sustainability. Geopolymer concrete with GBFS achieves compressive strengths of 60-70 MPa (Dinh et al., 2024), while FA and GBFS-stabilized soil shows a UCS of 5.1MPa (Sun et al., 2024). GBFS reduces microcracking under high temperatures (Sim et al., 2023) and increases material compactness by forming hydrated silicate gels (Sun et al., 2024). It also reduces carbon emissions compared to traditional cement (Wang et al., 2023). However, challenges like material variability and precise mixing ratios remain.

This study addresses the limited research on the use of medium-sized granulated blast furnace slag (GBFS) as a partial replacement for clay soil in Class F fly ash (FA) geopolymer stabilization for sustainable pavement applications. Although FA-GGBS geopolymer systems have been widely investigated for soil stabilization, previous studies have mainly focused on finely ground slag or conventional binder systems. The potential role of medium-sized GBFS particles (0.5-2 mm) as a partially reactive component in alkaline-activated soil stabilization, particularly in cement-free systems, has received limited attention. In addition, the combined influence of GBFS content, NaOH molarities, and curing duration on the mechanical and durability performance of FA-based geopolymer-stabilized clay soils has not been systematically examined. To address this gap, the present study evaluates unconfined compressive strength (UCS), tensile strength, and sulfate resistance by varying GBFS content (0, 5, 10, and 15% by weight of soil), NaOH molarity (4, 8, 12, and 16 M), and curing periods (7, 28, and 60 days). The findings aim to clarify the contribution of medium-sized GBFS in FA-based geopolymer stabilization and support its potential application in sustainable pavement subgrade improvement.

2. Experimental methodology

2.1. Materials characteristic of test

2.2.1 Soil

Soil samples were collected near Rajendra Bridge, Simaria, Begusarai, and the site location is shown in Figure 1.

The soil was classified as low-plasticity clay (CL) according toIS-1498 (BIS, 1970), the Indian Standard for soil classification. The liquid limit (33.19%) and plasticity index (18.18%) were determined following IS-2720(5) (BIS, 1985), which specifies procedures for liquid and plastic limit determination.

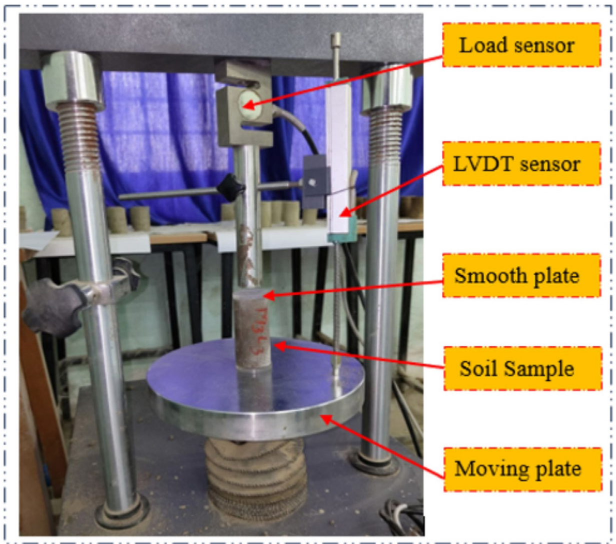

Figure 1. UCS test set up in laboratory.

The specific gravity of soil solids was found to be 2.43 using IS-2720(3) (BIS, 1980), the standard method for determining soil particle specific gravity, while the natural water content (13%) was determined in accordance with IS-2720(2) (BIS, 1973), the procedure for water content determination. Compaction characteristics were evaluated using IS-2720(8) (BIS, 1983), the standard Proctor compaction test, resulting in an optimum moisture content of 22.0% and a maximum dry density of 20.85 kN/m^3. The California Bearing Ratio (CBR) value of 12.7% was obtained following IS-2720(16) (BIS, 1987), which specifies the laboratory CBR test for evaluating subgrade strength.

The measured engineering properties of the clay soil, including CBR, were compared with the requirements for embankment and subbase materials specified in IRC-37 (IRC, 2018), the guideline for flexible pavement design, as summarized in Table 1. Although the soil does not satisfy the criteria for subbase materials under IRC 37-2018 (IRC, 2018), it meets the requirements for engineering fill, indicating that chemical stabilization may enable its effective utilization in remote construction projects.

2.2.2 Fly ash

Fly Ash (FA) was sourced from the NTPC plant in Barauni. The chemical composition of FA is presented in Table 2.

Table 1. Soil properties and sub-base material specifications.

Engineering properties	Soil sample	Subbase	
		Limits	Reference code
Liquid limit (LL) (%)	33.19	<35	IRC: SP:89 (IRC, 2010)
Plastic index (PI) (%)	18.18	<20	
California Bearing Ratio (CBR)	12.7	>20	IRC: SP-72-2015 (IRC, 1915)
UCS (MPa)	0.22	(0.75-1.5)	IRC: 37:2018 (IRC, 2018)

Table 2. Chemical compositions of fly ash, slag, and sodium silicate.

Composition (wt. %)	Fly ash	Slag	Sodium silicate
SiO_2	52.1	31.13	29.5
Na_2O	0.77	0.27	14.6
H_2O	-	-	55.9
Al_2O_3	21.56	10.1	-
Fe_2O_3	11.48	1.91	-
CaO	8.4	43.33	-
MgO	1.05	5.36	-
TiO_2	1.32	0.68	-
MnO	0.25	0.32	-
P_2O_5	0.885	0.13	-
K_2O	0.8	0.12	-
SO_3	0.25	4.31	-
Others	0.46	1.12	-
LOI	0.67	1.22	-

Note: LOI = Loss on ignition.

The primary constituents of the FA (SiO_2, Fe_2O_3, Al_2O_3) accounted for 70.44%, while the CaO content was 8.4%. Consequently, the FA was classified as low-calcium Class F.

2.2.3 Ground granulated blast furnace slag (GGBS)

Ground granulated blast furnace slag (GGBS) from JSC cement Chennai, India. The GGBS had a specific gravity of 2.89 and key chemical components: 32.4% SiO_2, 46.33% CaO, 10.43% Al_2O_3,1.91% Fe_2O_3 and 6.36% MgO (Table 2).

2.2.4 Alkali activator

The alkaline activator (AA) consisted of sodium silicate (Na_2SiO_3) and sodium hydroxide (NaOH) solutions. Na_2SiO_3 contained 15.50% Na_2O, 32.75% SiO_2, and 51.75% H_2O by weight. The NaOH solution, prepared 24 hours before use for safety, was made using distilled water.

2.3 Testing program

The experimental program assessed different soil mixes in terms of (1) compaction properties using standard Proctor test, (2) mechanical properties under unconfined compression, and indirect tensile strength test using split tensile test and (3) sulfate resistance of alkali-activated stabilized specimens.

2.3.1 Standard compaction test

The moisture content vs. dry density relationship for different soil mixes was determined using the standard Proctor test as per IS-4332(3) (BIS, 1967b), which specifies the procedure for determining compaction characteristics of stabilized soils. The moisture content of the compacted mixture was measured according to IS-4332(2) (BIS, 1967a), which provides the standard method for determining water content in stabilized soil mixtures. From this relationship, the optimum moisture content (OMC) and maximum dry density (MDD) were calculated.

2.3.2 Unconfined compression strength test

Unconfined compressive strength (UCS) testing was conducted as per IS-2720(10) (BIS, 1991), which outlines the laboratory procedure for determining the unconfined compressive strength of cohesive soils. Cylindrical specimens of 38 mm diameter and 76 mm height were prepared and tested. The experimental setup used for the UCS test is shown in Figure 1.

2.3.3. Split tensile test

Split tensile strength tests were conducted in accordance with IS-5816 (BIS, 1999), the standard test method for determining the splitting tensile strength of cylindrical specimens. The specimens were cured for 28 days prior to testing and were subjected to monotonic loading at a rate of 0.5 mm/min. The split tensile strength values were calculated using Equation 1, utilizing the peak loads recorded during the application of the load.

$$STS = \alpha x \frac{2 x P}{\pi x d x L} \tag{1}$$

here, *P* represents the maximum applied load, *d* and *L* denote the diameter and length of the specimen, respectively, and α is the shape parameter, expressed as α = (0.2621 k+1) where $k = L/D$ (Khaksar Najafi et al., 2021).

Cementitious materials, including soil cement, are highly vulnerable to sulfate attack, primarily due to chemical reactions that produce expansive minerals like ettringite and thaumasite, leading to swelling, heaving, and structural damage (Ramon-Tarragona and Alonso, 2020, Yi et al., 2020; Elahi et al., 2021). Soil cement deteriorates more rapidly than traditional cement concrete, with internal sulfate attack causing up to 70% strength loss and external attack reducing strength by about 20% (Atashband et al., 2020). Mitchell (1986) reported sulfate-induced heave in cement-stabilized soil subgrades due to soluble sodium sulfate (up to 1.5% by weight), while embankments treated with cement exhibited heaving rates of up to 4 mm/month (Ramon-Tarragona & Alonso, 2020). Long-term durability is often compromised, necessitating measures like underpinning to maintain structural integrity (Kalipcilar et al., 2018). Optimizing cement content and employing sulfate-resistant formulations have been suggested to mitigate these effects and improve resilience in sulfate-rich environments (Kampala et al., 2020).To evaluate sulfate resistance, alkali-activated stabilized clay soil specimens were cured for two weeks under ambient conditions, followed by immersion in a 5% sodium sulfate solution for an additional two weeks.

The UPV test is a non-destructive technique conducted to evaluate the primary wave velocity (V_p) and constrained modulus (G) of concrete and stabilized soils, following IS-13311(1) (BIS, 1992), which specifies the procedure for determining ultrasonic pulse velocity in concrete and similar materials.. In this method, two piezoelectric transducers are attached to opposite ends of a cylindrical specimen. The transmitter generates a primary wave, which travels through the sample and is received by the receiver transducer. The device records the travel time (ΔT) of the stress wave, and with the known travel path (X), the constrained modulus is calculated using Equation 2.

$$G = \rho V_P^2 = \rho \left(\frac{\mathrm{X}}{\Delta \mathrm{T}} \right)^2 \tag{2}$$

2.4 Sample preparations and casting

The soil was oven-dried at 105 °C for 24 hours, sieved through a 4.75 mm sieve (IS: 2720-Part 1), and mixed with 30% fly ash (FA) and varying GGBS contents (0%, 5%, 10%, and 15%) to prepare three soil mixes: SM0 (70:30:0), SM1 (65:30:5), SM2 (60:30:10), and SM3 (55:30:15) by weight. A Na_2SiO_3: NaOH (NS: NH) ratio of 70:30 was adopted for a cost-effective and strength-optimized design, as Phummiphan et al. (2016, 2017) indicated the optimal range is between 100:0 and 50:50. NaOH molarities of 4M, 8M,12M and 16M were used to investigate the effect of NaOH molarity on prepared soil mixes.

CL, FA, and GGBS were dry-mixed for 5 minutes (Figure 2), sprayed with alkaline activators (AA), and mixed further for 5 minutes. Standard Proctor tests determined the maximum dry density (MDD) and optimum moisture content (OMC), referred to as the optimum alkaline activator content (OAC).

For unconfined compressive strength (UCS) testing, CL, FA, and GGBS were again dry-mixed uniformly for 5 minutes and sprayed with AA equal to OAC, followed by additional mixing for 5 minutes. The mix was placed in cylindrical molds (38 mm diameter, 76 mm height) in three layers, each compacted with 25 blows from a 305.5 g rammer dropped from 247 mm. The compacted samples were extruded, wrapped in airtight plastic sheets to prevent moisture loss (Figure 2). For strength evaluation, specimens were cured under ambient laboratory conditions at 27 ± 2°C for 7, 28, and 60 days before UCS and tensile strength testing. For sulfate resistance assessment, a separate set of specimens was initially cured under ambient conditions for 7 days to allow early strength development, followed by immersion in a 5% Na_2SO_4 solution at 27 ± 2°C for 21 days. After sulfate exposure (total conditioning period: 28 days), specimens were surface-dried and UCS testing was conducted within 30 minutes. In total, 192 UCS samples were prepared for 16 soil mixes, with three samples tested for each curing condition to ensure accuracy. Detailed soil mix proportions naming and corresponding UCS sample counts are provided in Table 3.

The mix design was developed based on previous studies on FA-GGBS geopolymer soil stabilization, which reported that a fly ash content of about 30% provides sufficient aluminosilicate precursor for geopolymerization while maintaining workable mixtures in clayey soils. GGBS replacement levels of 0, 5, 10, and 15% by soil weight were selected to evaluate the influence of increasing calcium content on geopolymer reaction and strength development, while maintaining practical proportions for soil stabilization. The sodium silicate to sodium hydroxide (NS: NH) ratio of 70:30 was adopted from commonly used geopolymer formulations that provide adequate soluble silicate for gel formation and stable geopolymer networks. NaOH molarities of 4, 8, 12, and 16 M were selected to examine the effect of alkaline activation intensity on strength development, covering both moderate and relatively high activation levels typically reported in geopolymer-based soil stabilization. The entire preparation and compaction process were completed within 25 minutes, demonstrating suitability for rapid stabilization in pavement base and subbase applications.

3. Test results and discussions

3.1 Compaction behavior of FA/GGBS geopolymer-stabilized clay soil

As shown in Figure 3, the results indicate that increasing GGBS content from 0% (SM0) to 15% (SM3) reduces the optimum alkali content (OAC) and increases the maximum dry unit weight (MDUW), with the best results observed for 10% GGBS (SM2) and 15% GGBS (SM3) at 12M NaOH, achieving MDUW values of 17.96 kN/m^3 and 17.84 kN/m^3, respectively.

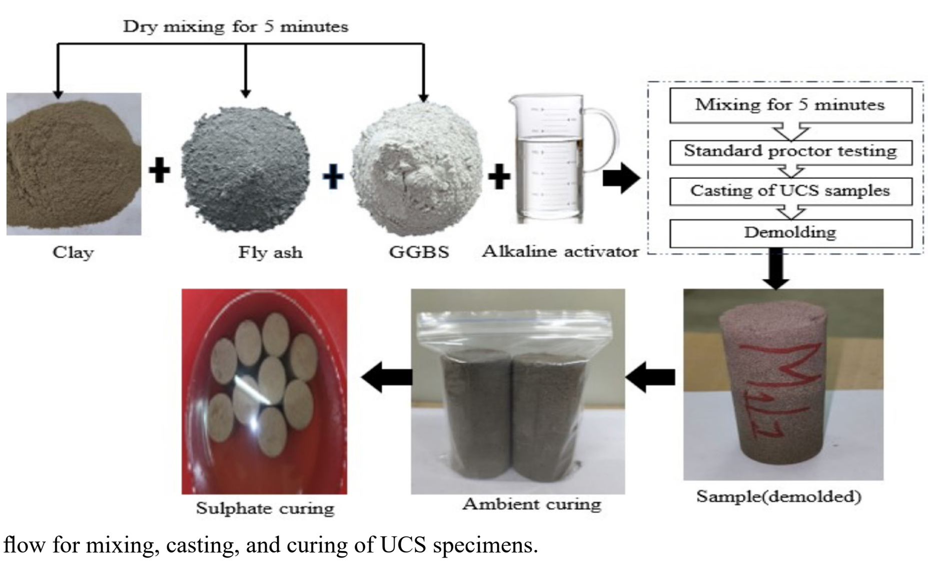

Figure 2. Process flow for mixing, casting, and curing of UCS specimens.

Table 3. Soil mix proportions, curing types, durations, and UCS sample counts.

Soil Mix Id	Clay Soil (%)	Fly ash (%)	GGBS (%)	NS: NH	NH Molarity	Curing days	No. of UCS samples
SM0NH04	70	30	0	70:30	4	[For all soil mix ids: ambient curing -7, 28, and 60 days; sulphate curing-14 days]	12
SM0NH08	70	30	0	70:30	8		12
SM0NH12	70	30	0	70:30	12		12
SM0NH16	70	30	0	70:30	16		12
SM1NH04	65	30	5	70:30	4		12
SM1NH08	65	30	5	70:30	8		12
SM1NH12	65	30	5	70:30	12		12
SM1NH16	65	30	5	70:30	16		12
SM2NH04	60	30	10	70:30	4		12
SM2NH08	60	30	10	70:30	8		12
SM2NH12	60	30	10	70:30	12		12
SM2NH16	60	30	10	70:30	16		12
SM3NH04	55	30	15	70:30	4		12
SM3NH08	55	30	15	70:30	8		12
SM3NH12	55	30	15	70:30	12		12
SM3NH16	55	30	15	70:30	16		12

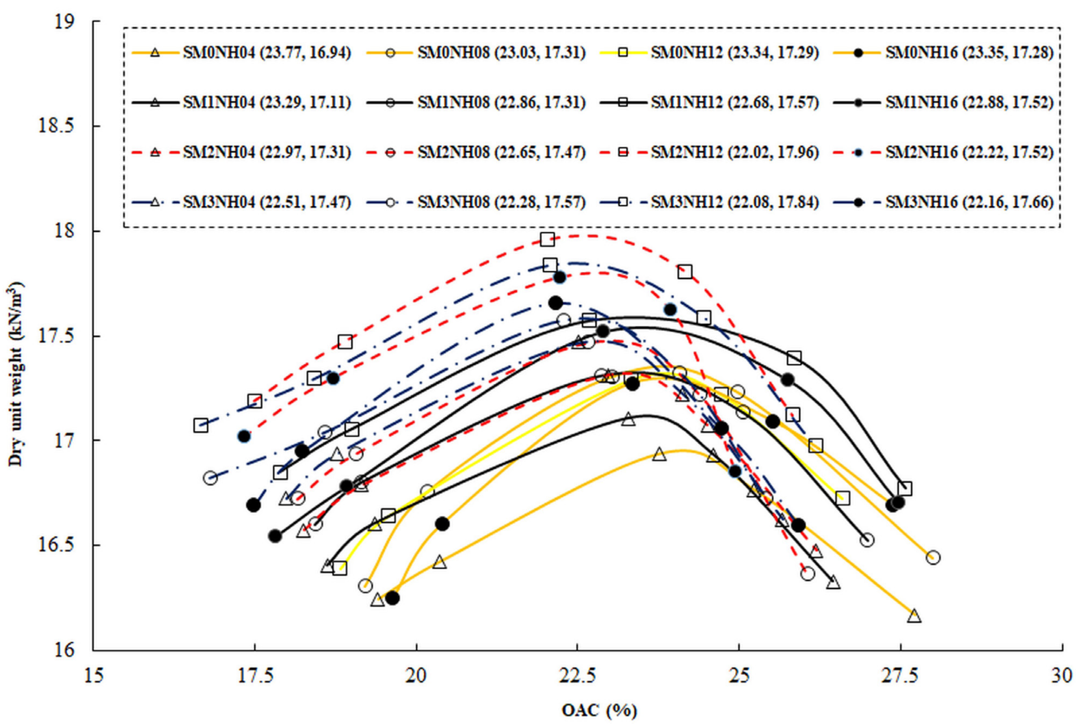

Figure 3. Compaction curves for soil mixes with 0-15% GGBS and 4M–16M NaOH.

The heavier particles of GGBS contribute to higher density, while the combination of fine fly ash and GGBS enhances particle packing, reducing voids during compaction. Additionally, pozzolanic reactions activated by NaOH improve particle bonding, particularly at 12M, resulting in better compaction and strength. These findings highlight that 10-15% GGBS with 12M NaOH provides the optimal balance for improved soil stabilization. Relationships between OAC and molarity of NaOH solutions for different soils mix are shown in Figure 4.

3.2 Unconfined compressive strength of FA/GGBS geopolymer-stabilized clay soil

3.2.1 Effect of NaOH concentrations

Figures 5 and 6 depict the stress-strain behavior of soil mixes containing varying ground granulated blast furnace slag (GGBS) contents (0%, 5%, 10%, and 15%)

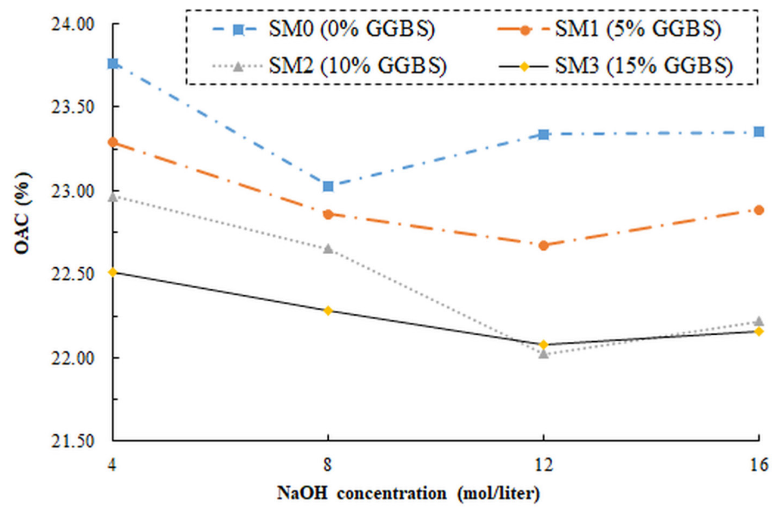

Figure 4. Relationship between OAC and molarity of NaOH for considered soil mixes.

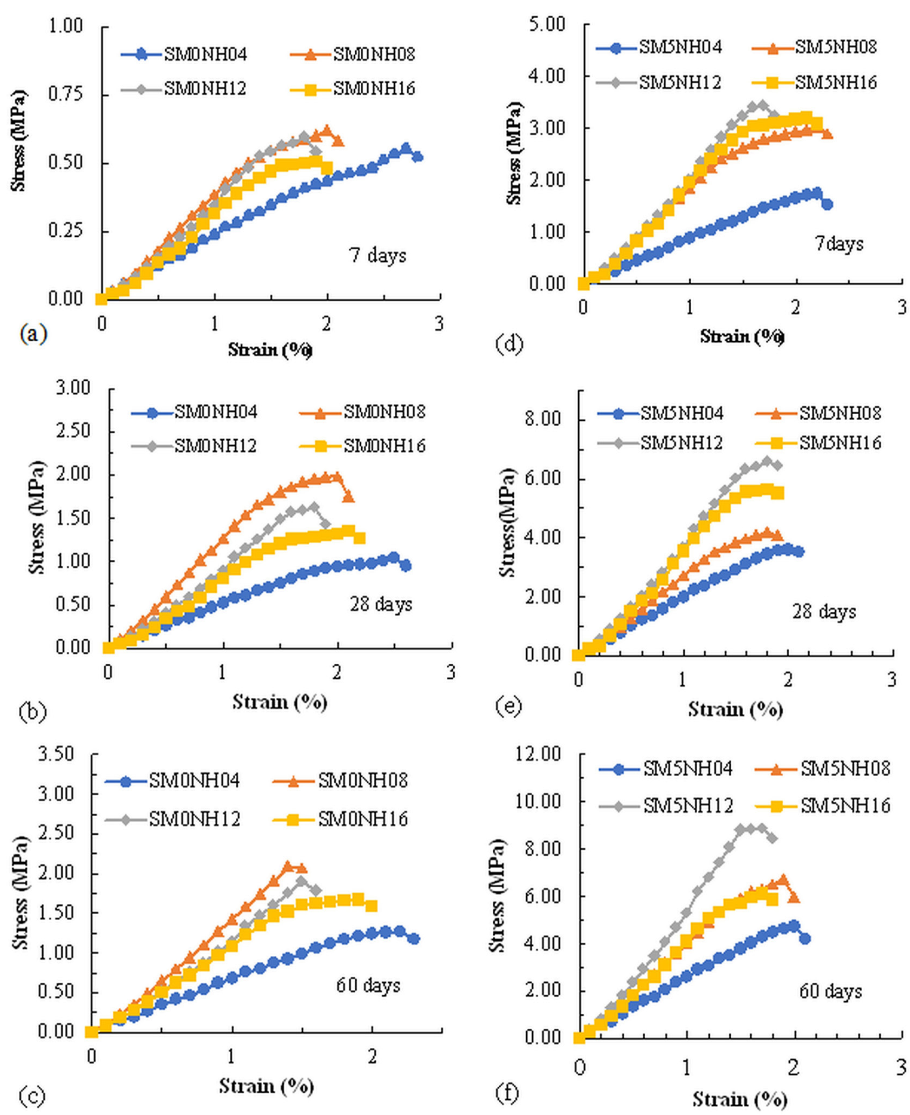

Figure 5. Stress-strain behaviors for SM0 soil (a-c) and SM1 soil (d-f) at 7, 28, and 60 days.

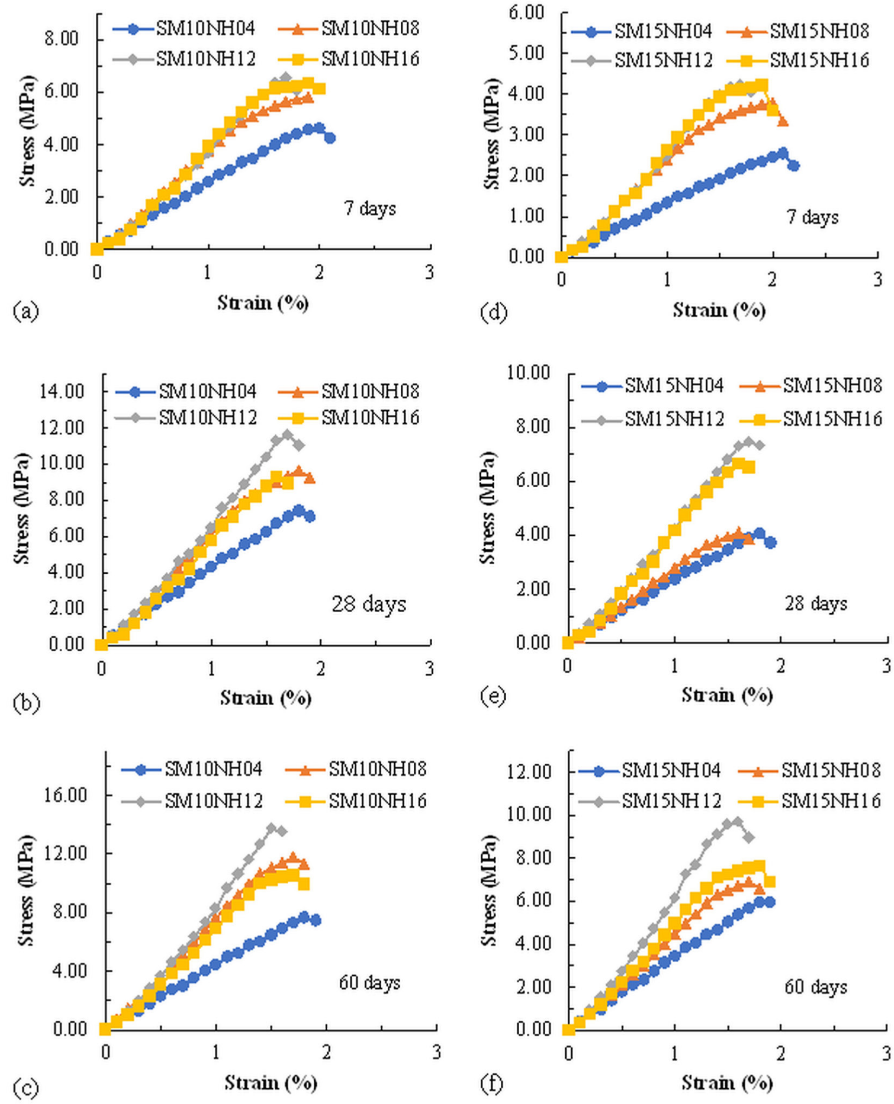

Figure 6. Stress-strain behaviors for SM2 soil (a-c) and SM3 soil (d-f) at 7, 28, and 60 days.

combined with 20% fly ash (FA) in all soil mixes (SM0: GGBS 0%, SM1: GGBS 5%, SM2: GGBS 10%, and SM3: GGBS 15%) under different NaOH concentrations (4M, 8M, 12M, and 16M) and ambient curing durations (7, 28, and 60 days). The progressive increase in stiffness and peak stress with curing time reflects the gradual development of geopolymeric binding phases within the soil matrix. Under alkaline activation, aluminosilicate precursors from FA and calcium-bearing phases from GGBS dissolve and reorganize to form geopolymer gels, primarily N–A–S–H gels derived from FA and C–(A)–S–H gels associated with the CaO content of GGBS (Wu et al., 2022). These reaction products are reported to progressively coat soil particles and fill interparticle voids, forming a cemented soil skeleton that enhances interparticle bonding and reduces pore spaces, as observed in previous microstructural studies on geopolymer-stabilized soils (Pourakbar et al., 2015; Khaksar Najafi et al., 2021). Consequently, the stress-strain curves exhibit steeper ascending branches and higher peak stresses with increasing curing duration. However, the reduction in failure strain with curing time indicates that the increasing dominance of rigid binding gels over the deformable clay matrix restricts particle rearrangement and promotes a more brittle response.

The influence of precursor composition and alkali concentration on strength development is summarized in Figures 7a-d. For SM0 (30% FA without GGBS), the UCS gradually increases with curing time and reaches a maximum value of 1.98 MPa at 8M NaOH after 60 days. The relatively moderate strength gain in this mix can be attributed to the lower reactivity of Class F FA, where geopolymerization proceeds slowly and produces a limited quantity of binding gels. Moderate alkali concentrations facilitate the dissolution of reactive silica and alumina species and promote geopolymer gel formation without destabilizing the developing matrix (Álvarez-Ayuso et al., 2008).

In contrast, the incorporation of GGBS significantly enhances strength development in mixes SM1-SM3. The calcium-rich nature of GGBS promotes the formation of additional C–(A)–S–H type gels alongside N–A–S–H structures, which has been widely reported to produce a denser and more cohesive microstructure in geopolymer systems (Álvarez-Ayuso et al., 2008; Khater, 2014). As a result, higher UCS values are obtained, with optimal performance observed at 12M NaOH (SM2: 13.62 MPa, SM3: 9.69 MPa, and SM1: 8.8 MPa after 60 days). The improved strength can be attributed to enhanced dissolution of reactive species and more extensive gel formation, which effectively binds soil particles and fills internal voids. However, a decline in UCS at 16M NaOH suggests that excessive alkalinity may destabilize the geopolymeric system, potentially leading to incomplete gel formation or microstructural defects that limit further strength development (Khater, 2014).

The failure patterns shown in Figure 8 further illustrate the evolution of the soil structure during curing. At early curing stages (7 days), the specimens exhibit relatively ductile behavior characterized by localized cracking and gradual deformation, indicating that geopolymerization is still incomplete and the soil matrix retains some clay-controlled plasticity.

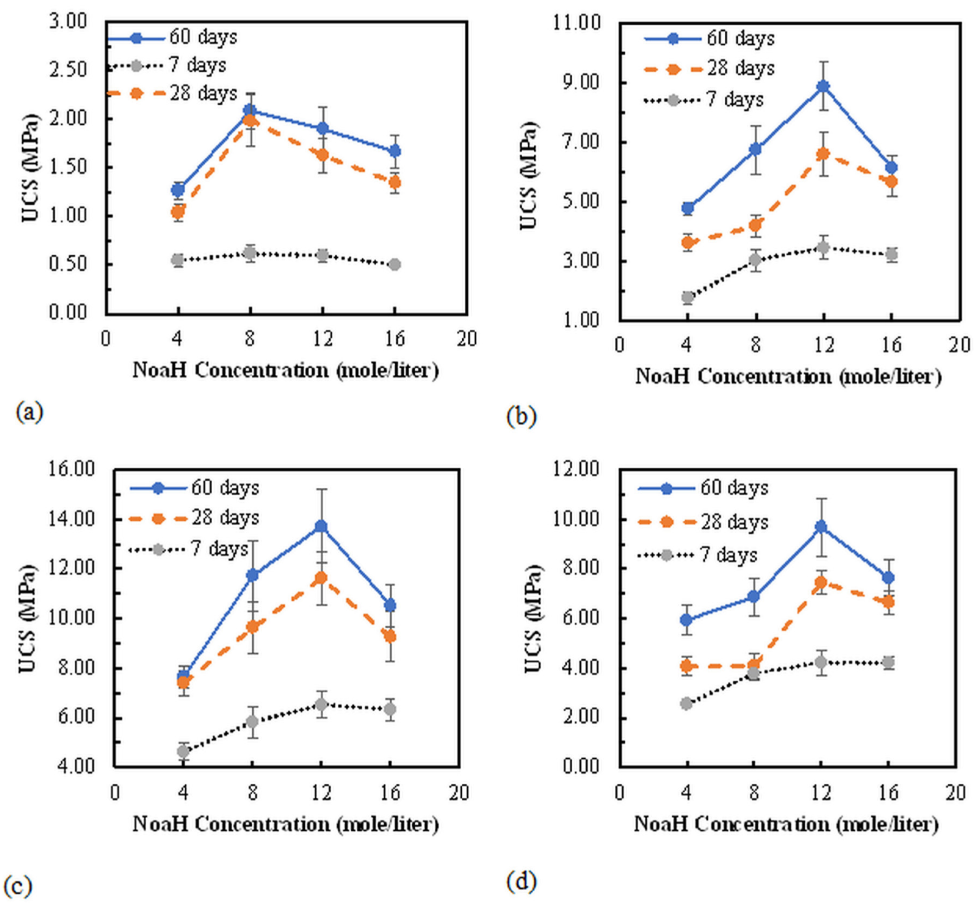

Figure 7. UCS response with NaOH concentrations for (a) SM0, (b) SM1, (c) SM2, and (d) SM3 at 7, 28, and 60 days.

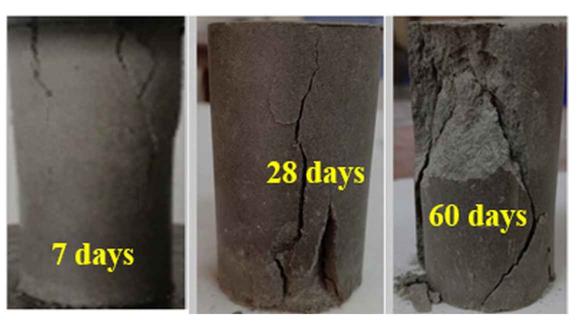

Figure 8. Crack patterns observed in SM2NH12 specimens at 7 days, 28 days, and 60 days.

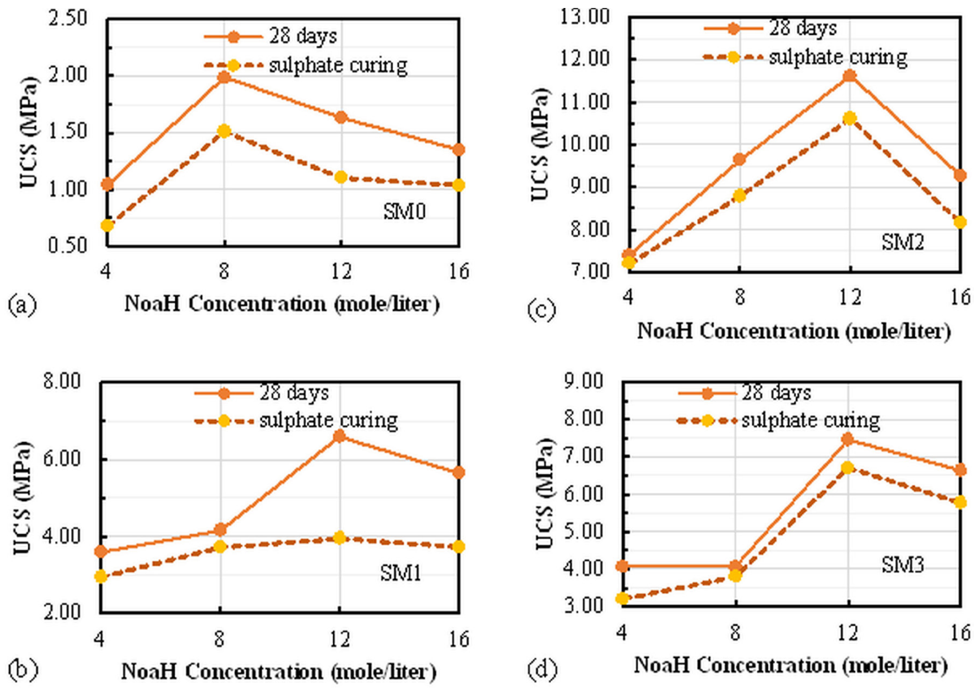

Figure 9. UCS response with NaOH concentrations for (a) SM0, (b) SM1, (c) SM2, and (d) SM3 under 28 days ambient curing and 28 days sulfate curing.

With extended curing (28-60 days), continued gel formation and pore refinement produce a denser and more rigid matrix that significantly enhances strength but reduces deformability. Consequently, the failure mode shifts toward brittle behavior, characterized by distinct shear cracks propagating along the specimen length and a sharp post-peak stress drop. This transition from ductile to brittle response reflects the transformation of the soil structure from a deformable clay-dominated system into a strongly cemented geopolymer-stabilized matrix, consistent with the microstructural evolution reported for geopolymer materials in previous studies (Kashani et al., 2017; Qian et al., 2025).

3.2.2 Effect of sulphate

The sulphate resistance of soil mixes, as shown in Figures 9a-d, was evaluated based on the percentage drop in UCS for samples subjected to ambient curing for 28 days and those cured under 1 week of normal conditions followed by 3 weeks of sulphate exposure (total 28 days). SM0 exhibited the highest percentage drop in UCS (34.62% at 4M and 24.12% at 8M), indicating poor sulphate resistance due to the absence of GGBS. SM1 (GGBS 5%) showed moderate resistance, with UCS reductions ranging from 18.05% (4M) to 40.15% (16M). SM2 demonstrated the highest sulphate resistance, with minimal UCS drops (2.83% at 4M and 8.68% at 12M), attributed to the optimal GGBS content enhancing durability and mitigating sulphate-induced degradation. SM3 exhibited good resistance, with percentage reductions ranging from 21.12% (4M) to 10.06% (12M), although slightly less effective than SM2 (GGBS 10%) due to potential over-saturation effects at higher GGBS levels. These findings align with Khater (2014), who reported a reduction in the strength of slag-based geopolymer mortar under sulphate exposure. This confirms that sulphate resistance improves with increasing GGBS content, with 12M NaOH proving most effective in achieving durability against sulphate exposure.

3.3 Split tensile strength (STS) of FA/GGBS geopolymer-stabilized clay soil

At 28 days (Figure 10), the STS of soil mixes (SM0 to SM3) follows trends similar to UCS, increasing with NaOH molarity up to 12M before declining at 16M. SM0 (0% GGBS) consistently exhibits the lowest strength, highlighting the contribution of GGBS to matrix development. SM2 (10% GGBS) achieves the highest STS, with a peak of 4.04 MPa at 12M. These results emphasize the influence of both NaOH concentration and GGBS content on enhancing the tensile performance of geopolymer soil mixes under ambient curing conditions.

3.4 Constrained modulus (*G*) of FA/GGBS geopolymer-stabilized clay soil

Figures 11a-d illustrate the variation of constrained modulus (*G*) with NaOH concentration for four soil mixtures at different curing times. The constrained modulus of all alkali-activated specimens increases with curing age, following a similar trend to the UCS and split tensile strength (STS), with the highest stiffness values observed in the SM0 to SM03 samples.

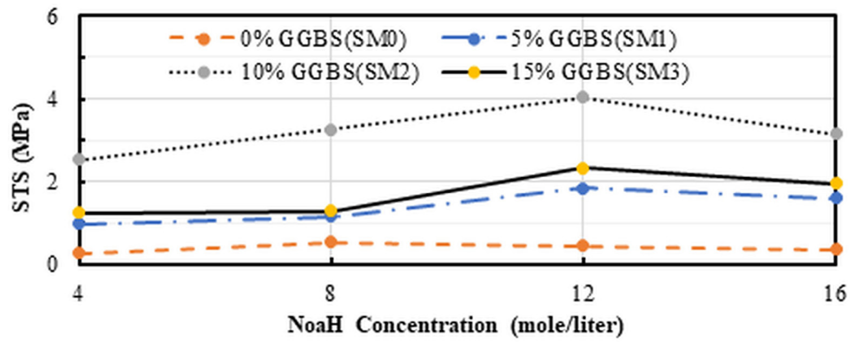

Figure 10. STS response with NaOH concentrations for soils SM0, SM1, SM2, and SM3 at 28 days.

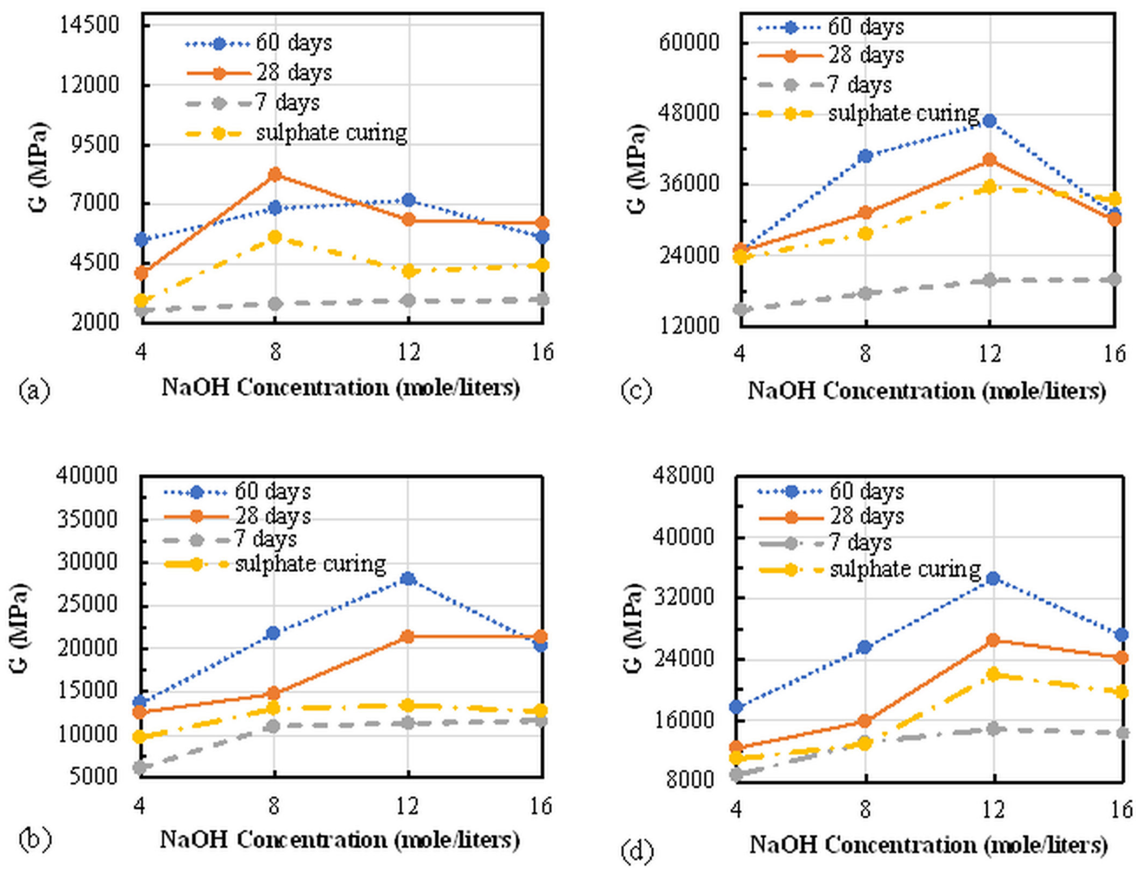

Figure 11. Behavior of constrained modulus with NaOH concentration for (a) SM0; (b) SM01; (c) SM02; and (d) SM03 soil mixes.

3.5 Relationship between UCS and constrained modulus (*G*)

To better understand and predict the geotechnical behavior of treated CL soils, establishing direct correlations between their strength and stiffness properties is of significant practical value. Such correlations allow for the estimation of one mechanical parameter from the other. As discussed in previous sections, the stiffness and compressive strength of alkali-activated clays exhibit similar improvement trends with increasing NaOH concentration and curing time. The strength and stiffness values of the four treated clay samples (SM0-SM03: GGBS 0-15%) are plotted in Figure 12. Linear regression was applied to the data sets, generating best-fit lines to establish a general relationship between the UCS and constrained modulus (*G*) of these mixtures. From Figure 12, a strong correlation between UCS and *G* is observed, with a correlation coefficient (R^2) of 0.98. The developed correlation equation is shown in Equation 3, demonstrating the established relationship between the two parameters.

$$G = 3281.5UCS + 629.44 \quad (3)$$

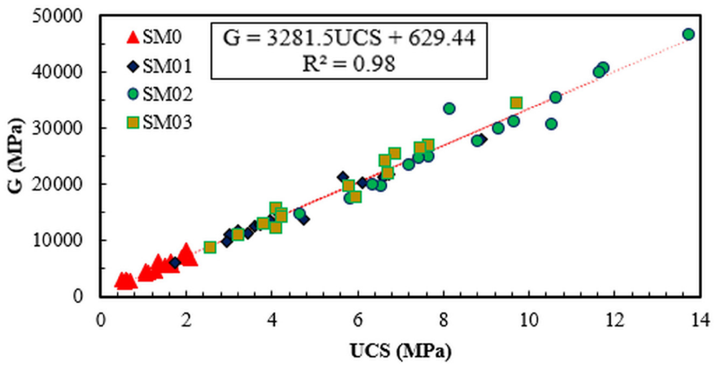

Figure 12. Correlation between UCS and constrained modulus (*G*).

It should be noted that the developed correlation is empirical and derived from the experimental data obtained in this study under specific conditions, including the investigated ranges of NaOH concentration, curing duration, and FA–GGBS contents. Therefore, the proposed relationship is primarily applicable to similar geopolymer-stabilized CL soils within the studied parameter range. Variations in soil mineralogy, binder composition, activator chemistry, or curing conditions may influence the strength–stiffness relationship and could lead to deviations from the proposed model. Additional datasets and broader statistical evaluation would further improve the general applicability and reliability of the correlation.

4. Sustainability assessment

To substantiate the sustainability claims of the proposed FA–GGBS geopolymer stabilization system, a comprehensive environmental assessment was carried out incorporating both absolute carbon emissions and performance-based evaluation. Unlike conventional approaches that assume fixed binder content, the present study utilizes experimentally determined optimum alkali content (OAC) for each mix, expressed as a percentage of the total mix (soil + fly ash + GGBS), thereby providing a more realistic representation of field conditions.

4.1 Carbon emission assessment

A comparative carbon emission analysis was performed between conventional ordinary Portland cement (OPC)-based stabilization and the proposed geopolymer system. For reference, a typical OPC dosage of 10% by dry weight of soil was considered, which is widely adopted in pavement and subgrade stabilization practices (Ghosh & Subbarao, 2007). The emission factor for OPC was taken as 0.85–0.95 kg CO_2/kg, reflecting the high energy demand associated with clinker production(Andrew, 2018; Scrivener et al., 2018).

In contrast, the geopolymer system utilizes industrial by-products such as fly ash (FA) and ground granulated blast furnace slag (GGBS), which exhibit significantly lower embodied carbon, typically 0.02–0.05 kg CO_2/kg for FA and 0.07–0.10 kg CO_2/kg for GGBS (Habert et al., 2011; Turner & Collins, 2013). However, the overall environmental performance is strongly influenced by the alkaline activators. Sodium hydroxide (NaOH) has an emission factor of approximately 1.1-1.5 kg CO_2/kg, while sodium silicate (Na_2SiO_3) ranges between 0.8-1.2 kg CO_2/kg, due to energy-intensive manufacturing processes (Turner & Collins, 2013).

In this study, the total activator content was determined from the OAC values (≈22-24%) for each mix and subsequently divided into NaOH and Na_2SiO_3 using a fixed ratio of NS:NH = 70:30. The resulting CO_2 emissions for the geopolymer mixes were found to range between 218 and 236 kg CO_2 per m^3 (Table 4), which are higher than the OPC reference system (~90 kg CO_2).

This outcome highlights that while geopolymer systems eliminate clinker-related emissions, the high dosage of alkaline activators, particularly sodium silicate, dominates the carbon footprint. Similar observations have been reported in previous studies, which indicate that alkaline activators can contribute up to 60–80% of total emissions in geopolymer systems (Habert et al., 2011; Turner & Collins, 2013).

4.2 Performance-based sustainability evaluation

To overcome the limitations of direct emission comparison, a performance-based sustainability assessment was conducted by normalizing CO_2 emissions with respect to unconfined compressive strength (UCS). A CO_2 efficiency index (kg CO_2 per MPa) was adopted to evaluate environmental performance per unit strength.

The results (Figure 13) demonstrate a significant reduction in CO_2/UCS values with increasing GGBS content up to 10%, indicating improved environmental efficiency. The optimum performance was observed for the mix containing 10% GGBS at 12M NaOH concentration, which exhibited the lowest CO_2/UCS value (~19.2 kg CO_2/MPa), representing the best balance between strength development and environmental impact.

Table 4. Comparative CO_2 emissions of FA–GGBS geopolymer mixes calculated using mix-specific optimum alkali content (OAC), expressed as a percentage of total mix (soil + FA + GGBS), for a reference total mix mass of 1000 kg and activator ratio NS:NH = 70:30.

Mix ID	GGBS (%)	NaOH M	OAC (%)	NaOH (kg/m³)	Na_2SiO_3 (kg/m³)	CO_2 (kg/m³)
SM0NH04	0	4	23.77	71.3	166.4	224.5
SM0NH08	0	8	23.03	69.1	161.2	218.1
SM0NH12	0	12	23.34	70.0	163.4	221.0
SM0NH16	0	16	23.35	70.1	163.5	221.1
SM1NH04	5	4	23.29	69.9	163.0	228.0
SM1NH08	5	8	22.86	68.6	160.0	223.6
SM1NH12	5	12	22.68	68.0	158.8	221.9
SM1NH16	5	16	22.88	68.6	160.2	223.9
SM2NH04	10	4	22.97	68.9	160.8	232.0
SM2NH08	10	8	22.65	67.9	158.6	228.6
SM2NH12	10	12	22.02	66.1	154.1	222.8
SM2NH16	10	16	22.22	66.7	155.5	224.6
SM3NH04	15	4	22.51	67.5	157.6	236.0
SM3NH08	15	8	22.28	66.8	155.9	233.8
SM3NH12	15	12	22.08	66.2	154.6	232.1
SM3NH16	15	16	22.16	66.5	155.1	232.8

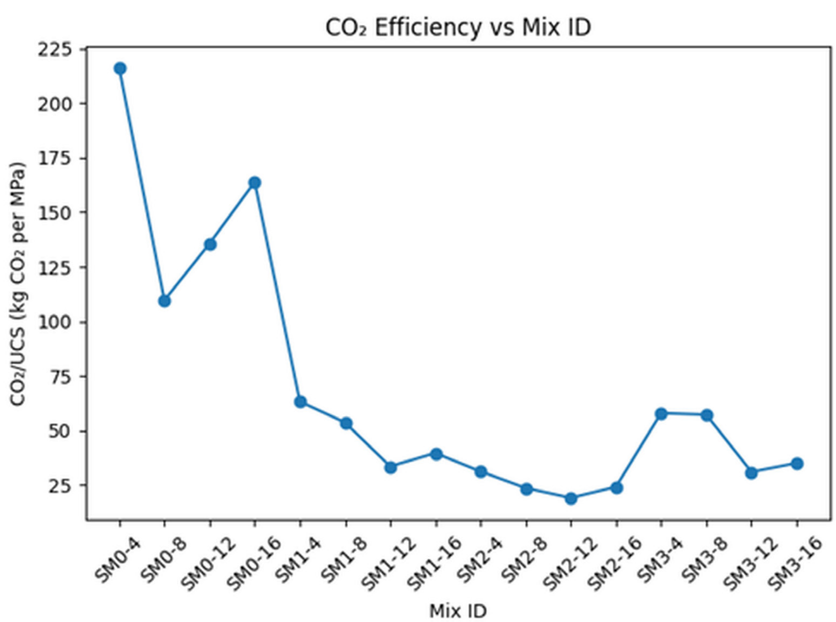

Figure 13. Variation of CO_2 efficiency (kg CO_2 per MPa) for different FA–GGBS geopolymer mixes based on OAC.

Beyond this level, further increase in GGBS content (15%) did not improve sustainability due to marginal strength gain combined with increased activator demand. These findings clearly indicate that absolute CO_2 emissions alone do not provide a complete picture of sustainability, and performance-based normalization is essential for realistic evaluation.

The present analysis highlights two key aspects:

- Activator Dominance: The environmental impact of geopolymer systems is primarily governed by alkaline activators, particularly sodium silicate;
- Need for Optimization: Sustainable geopolymer design requires optimization of activator dosage and binder composition.

It is also important to note that simplified carbon calculations may overestimate emissions, as industrial by-products such as FA and GGBS are often assigned negligible environmental burden in allocation-based life cycle assessment frameworks (Scrivener et al., 2018). Additionally, the geopolymer system demonstrated improved mechanical performance and sulfate resistance, which can enhance durability and reduce long-term maintenance, thereby contributing to sustainability over the service life. Recent studies further emphasize that the environmental viability of geopolymer systems depends on reducing activator intensity and developing low-carbon alternatives, rather than solely relying on precursor substitution.

Overall, the results demonstrate that while FA–GGBS geopolymer stabilization may exhibit higher absolute CO_2 emissions due to activator usage, its environmental performance improves significantly when evaluated on a strength-normalized basis. The study establishes that 10% GGBS with optimized alkali concentration (12M) provides the most sustainable mix, balancing mechanical performance and environmental impact.

5. Conclusions

This study investigated the viability of using class F fly ash (FA) and ground granulated blast furnace slag (GGBS) as industrial by-products in the geopolymer stabilization of lean clay soil (CL) for enhanced mechanical performance. The effects of NaOH concentration, GGBS content, and curing duration on strength and durability properties were systematically analyzed to optimize the geopolymerization process. Mechanical properties were evaluated using unconfined compressive strength (UCS), split tensile strength (STS), and ultrasonic pulse velocity (UPV), and durability was assessed through sulphate resistance tests. The key findings and practical implications are summarized as follows:

- The UCS of FA–GGBS stabilized soils improved with increasing NaOH molarity up to 12 M and with curing duration up to 60 days. Among the investigated mixes, SM2 (10% GGBS) exhibited the highest UCS of 13.62 MPa at 12 M NaOH after 60 days of curing, followed by SM3 (15% GGBS) and SM1 (5% GGBS). A slight reduction in UCS was observed at 16 M NaOH, likely due to excessive alkalinity affecting the geopolymerization process;
- The failure mode of stabilized specimens evolved from ductile behavior at early curing (7 days) to brittle failure at longer curing periods (28–60 days), reflecting progressive geopolymer matrix development and increased stiffness;
- Sulphate resistance improved with increasing GGBS content, with SM2 (10% GGBS) showing the best durability performance. Under sulphate exposure, UCS reductions were limited to 2.83% at 4 M NaOH and 8.68% at 12 M NaOH, whereas SM0 (0% GGBS) exhibited the highest strength reduction (34.62% at 4 M NaOH), highlighting the role of GGBS in enhancing durability under sulphate attack;
- Split tensile strength increased with NaOH molarity up to 12 M for all mixes. The maximum STS value of 4.04 MPa was obtained for SM2 at 12 M NaOH under 28-day ambient curing, demonstrating the synergistic contribution of NaOH concentration and GGBS content to tensile performance;
- The constrained modulus (G) increased with curing duration and followed trends similar to UCS and STS. A strong linear relationship between UCS and G (R^2 = 0.98) was established for the investigated mixtures, enabling practical estimation of stiffness from strength data within the studied material composition and curing conditions;
- The sustainability assessment indicates that although geopolymer mixes exhibit higher absolute CO_2 emissions due to the contribution of alkaline activators, their environmental efficiency improves significantly when evaluated on a strength-normalized basis (CO_2/UCS). The optimum mix (10% GGBS with 12M NaOH) demonstrates the lowest CO_2/UCS ratio, indicating the most favorable balance between mechanical performance and environmental impact.

These findings underline the potential of FA-GGBS-based geopolymer stabilization for pavement applications, offering a sustainable alternative to traditional cement stabilization. The enhanced strength, durability, and tensile performance demonstrate its suitability for geotechnical applications in sulphate-prone environments, while the developed strength-stiffness correlations provide valuable tools for geotechnical design and performance assessment.

5.1 Future research

The present study focuses on the engineering performance of FA-GGBS geopolymer-stabilized soils; however, further investigation is required to better understand the underlying mechanisms. Advanced microstructural and chemical characterization techniques such as SEM and FTIR should be employed to identify reaction products and correlate microstructure with strength and durability. In addition, future work should focus on optimizing alkali activator dosage, exploring low-carbon alternatives, and conducting detailed life cycle assessment (LCA) to comprehensively evaluate environmental performance.

Acknowledgements

The authors gratefully acknowledge the financial support provided by RRSDCE Begusarai.

Declaration of interest

The authors have no conflicts of interest to declare.

Authors' contributions

Lakshmi Kant: conceptualization, methodology, data curation, formal analysis, visualization, writing – original draft, supervision. Sanjeet Kumar: investigation, methodology, validation, writing – review & editing. Md Asfaque Ansari: writing – review & editing. Sunny Raj: investigation, experimental work, data curation.

Data availability

The data that support the findings of this study are available from the corresponding author upon reasonable request.

Declaration of use of generative artificial intelligence

This work was prepared without the use or assistance of any generative artificial intelligence (GenAI) tools or services. All aspects of the manuscript were developed solely by the authors, who take full responsibility for the content of this publication.

List of symbols and abbreviations

d	Diameter of the specimen
AA	Alkali activator
CASH	Calcium silicate hydrate
CBR	California bearing ratio
CCR	Calcium carbide residue
CL	Lean clay
CO_2	Carbon dioxide
CSH	Calcium silicate hydrate
FA	Fly ash
G	Constrained modulus
GBFS	Granulated blast-furnace slag
GGBS	Ground granulated blast-furnace slag
IRC	Indian roads congress
IS	Indian standard
L	Length of the specimen
LL	Liquid limit
LOI	Loss on ignition
MDD	Maximum dry density
NASH	Sodium aluminosilicate hydrate
NS	Sodium silicate
NH	Sodium hydroxide
OAC	Optimum alkali content
OMC	Optimum moisture content
P	Maximum applied load
PL	Plastic limit
R^2	Correlation coefficient
RHA	Rice husk ash
SM	Soil mix
SP	Special publication
STS	Split tensile strength
UCS	Unconfined compressive strength
UPV	Ultra pulse velocity
V_p	Primary wave velocity
X	Travel path
α	Shape parameter
ρ	Mass density
ΔT	Travel time

References

Abu Bakar, M.S., Manar, G., Syamsir, A., Abdul Rahman, M.R., Saad, M.R., Najeeb, M.I., Alhayek, A., & Muhammad Asyraf, M.R. (2024). An overview of fly-ash geopolymer composites in sustainable advance construction materials. *Pertanika Journal of Science & Technology*, 32(S5), 75-102. https://doi.org/10.47836/pjst.32.S5.04.

Ahmad, W., Ahmad, A., Ostrowski, K.A., Aslam, F., & Joyklad, P. (2021). A scientometric review of waste material utilization in concrete for sustainable construction. *Case Studies in Construction Materials*, 15, e00683. https://doi.org/10.1016/j.cscm.2021.e00683.

Al Khafaji, A.E., Waily, M.J., & Jawad, Z.F. (2024). Strength performance of soft clayey soil solidified by slag- fly ash – metakaolin based geopolymer. *IOP Conference Series: Earth and Environmental Science*, 1374, 012020. Retrieved in December 11, 2025, from https://iopscience.iop.org/article/10.1088/1755-1315/1374/1/012020

Álvarez-Ayuso, E., Querol, X., Plana, F., Alastuey, A., Moreno, N., Izquierdo, M., Font, O., Moreno, T., Diez, S., Vázquez, E., & Barra, M. (2008). Environmental, physical and structural characterisation of geopolymer matrixes synthesised from coal (co-) combustion fly ashes. *Journal of Hazardous Materials*, 154(1-3), 175-183. https://doi.org/10.1016/j.jhazmat.2007.10.008.

Amiri, M., Sanjari, M., & Porhonar, F. (2022). Microstructural evaluation of the cement stabilization of hematite-rich red soil. *Case Studies in Construction Materials*, 16, e00935. https://doi.org/10.1016/j.cscm.2022.e00935.

Amnadnua, K., Tangchirapat, W., & Jaturapitakkul, C. (2013). Strength, water permeability, and heat evolution of high strength concrete made from the mixture of calcium carbide residue and fly ash. *Materials & Design*, 51, 894-901. https://doi.org/10.1016/j.matdes.2013.04.099.

Andavan, S., & Pagadala, V.K. (2020). A study on soil stabilization by addition of fly ash and lime. *Materials Today: Proceedings*, 22, 1125-1129. https://doi.org/10.1016/j.matpr.2019.11.323.

Andrew, R. (2018). Global CO_2 emissions from cement production. *Earth System Science Data*, 10(1), 195-217. Retrieved in December 11, 2025, from https://essd.copernicus.org/articles/11/1675/2019/

Ansari, M.A., Roy, L.B., & Kumar, S. (2024). Performance of geocell reinforced rubber sand mixtures under undrained triaxial test. *Soils and Rocks*, 47(4), e2024001024. https://doi.org/10.28927/SR.2024.001024.

Arulrajah, A., Kua, T.-A., Phetchuay, C., Horpibulsuk, S., Mahghoolpilehrood, F., & Disfani, M.M. (2016). Spent coffee grounds-fly ash geopolymer used as an embankment structural fill material. *Journal of Materials in Civil Engineering*, 28(5), 04015197. https://doi.org/10.1061/(ASCE)MT.1943-5533.0001496.

Astuti, P. (2024). The mechanical performance evaluation of fly-ash derived geopolymer mortar for concrete patch repair. *Multidisciplinary Science Journal*, 7(3), 2025161. https://doi.org/10.31893/multiscience.2025161.

Atashband, S., Sabermahani, M., & Elahi, H. (2020). Internal and external effects of sodium sulfate on the strength of soil cement. *Civil Engineering*, 45(4), 2595-2610. https://doi.org/10.1007/s40996-020-00459-w.

Bagheri, A., & Nazari, A. (2014). Compressive strength of high strength class C fly ash-based geopolymers with reactive granulated blast furnace slag aggregates designed by Taguchi method. *Materials & Design*, 54, 483-490. https://doi.org/10.1016/j.matdes.2013.07.035.

Bernal, S.A., Provis, J.L., Provis, J.L., Walkley, B., Nicolas, R.S., Gehman, J.D., Brice, D.G., Kilcullen, A.R., Duxson, P., & Deventer, J.S.J. (2013). Gel nanostructure in alkali-activated binders based on slag and fly ash, and effects of accelerated carbonation. *Cement and Concrete Research*, 53, 127-144. https://doi.org/10.1016/j.cemconres.2013.06.007.

Bezerra, G., Bertoco, M.S., Reis, J.H.C., & Lukiantchuki, J.A. (2025). Effect of quarry dust (QD) particle on the strength, durability, and microstructure of lime stabilized lateritic sandy soil. *Soils and Rocks*, 49(1), e2026009224. https://doi.org/10.28927/SR.2026.009224.

BIS IS-4332(2). (1967a). *Methods of test for stabilized soils.* Bureau of Indian Standards, New Delhi.

BIS IS-4332(3). (1967b). *Methods of test for stabilized soils.* Bureau of Indian Standards, New Delhi.

BIS IS-1498. (1970). *Classification and identification of soils for general engineering purposes.* Bureau of Indian Standards, New Delhi.

BIS IS-2720(2). (1973). *Methods of tests for soils.* Bureau of Indian Standards, New Delhi.

BIS IS-2720(3). (1980). *Methods of tests for soils.* Bureau of Indian Standards, New Delhi.

BIS IS-2720(8). (1983). *Methods of tests for soils.* Bureau of Indian Standards, New Delhi.

BIS IS-2720(5). (1985). *Methods of tests for soils.* Bureau of Indian Standards, New Delhi.

BIS IS-2720(16). (1987). *Methods of tests for soils.* Bureau of Indian Standards, New Delhi.

BIS IS-2720(10). (1991). *Methods of tests for soils.* Bureau of Indian Standards, New Delhi.

BIS IS-13311(1). (1992). *Non destructive testing of concrete: method of test.* Bureau of Indian Standards, New Delhi.

BIS IS-5816. (1999). *Splitting tensile strength of concrete: method of test.* Bureau of Indian Standards, New Delhi.

Consoli, N.C., Párraga Morales, D., & Saldanha, R.B. (2021). A new approach for stabilization of lateritic soil with Portland cement and sand: strength and durability. *Acta Geotechnica*, 16(5), 1473-1486. https://doi.org/10.1007/s11440-020-01136-y.

Davidovits, J. (1994). Global warming impact on the cement and aggregates industries. *World Resource Review*, 6(2), 263-278.

Davidovits, J. (2013). *Geopolymer cement: a review* (Technical Papers, No. 21, pp. 1-11). Geopolymer Institute.

Dinh, H.L., Liu, J., Doh, J.H., & Ong, D.E.L. (2024). Influence of Si/Al molar ratio and ca content on the performance of fly ash-based geopolymer incorporating waste glass and GGBFS. *Construction & Building Materials*, 411, 134741. https://doi.org/10.1016/j.conbuildmat.2023.134741.

Duxson, P., Provis, J.L., Lukey, G.C., & Van Deventer, J.S. (2007). The role of inorganic polymer technology in the development of 'green concrete'. *Cement and Concrete Research*, 37(12), 1590-1597. https://doi.org/10.1016/j.cemconres.2007.08.018.

Elahi, M.A., Shearer, C.R., Naser Rashid Reza, A., Saha, A.K., Khan, M.N.N., Hossain, M.A., & Sarker, P.K. (2021). Improving the sulfate attack resistance of concrete by using supplementary cementitious materials (SCMs): a review. *Construction & Building Materials*, 281, 122628. https://doi.org/10.1016/j.conbuildmat.2021.122628.

Gajghate, V., & Nardey, D.A. (2024). Mechanical characters of geo-polymer concrete for major alteration of cement by fly ash. *Panamerican Mathematical Journal*, 34(4), 1. https://doi.org/10.52783/pmj.v34.i4.1881.

Ghosh, A., & Subbarao, C. (2007). Strength characteristics of class F fly ash modified with lime and gypsum. *Journal of Geotechnical and Geoenvironmental Engineering*, 133(7), 757-766. https://doi.org/10.1061/(ASCE)1090-0241(2007)133:7(757).

Guo, X., Shi, H.-S., Chen, L., & Dick, W.A. (2010). Alkali-activated complex binders from class C fly ash and Ca-containing admixtures. *Journal of Hazardous Materials*, 173(1-3), 480-486. https://doi.org/10.1016/j.jhazmat.2009.08.110.

Habert, G., De Lacaillerie, J.D.E., & Roussel, N. (2011). An environmental evaluation of geopolymer based concrete production: reviewing current research trends. *Journal of Cleaner Production*, 19(11), 1229-1238. https://doi.org/10.1016/j.jclepro.2011.03.012.

Handayani, L., Aprilia, S., Abdullah, Rahmawati, C., Aulia, T.B., Ludvig, P., & Ahmad, J. (2022). Sodium silicate from rice husk ash and their effects as geopolymer cement. *Polymers*, 14(14), 2920. https://doi.org/10.3390/polym14142920.

Hoy, M., Rachan, R., Horpibulsuk, S., Arulrajah, A., & Mirzababaei, M. (2017). Effect of wetting–drying cycles on compressive strength and microstructure of recycled asphalt pavement: fly ash geopolymer. *Construction & Building Materials*, 144, 624-634. https://doi.org/10.1016/j.conbuildmat.2017.03.243.

Humbal, A., Chaudhary, N. & Pathak, B. (2023). *Urbanization trends, climate change, and environmental sustainability* (pp. 151-166). Singapore: Springer. https://doi.org/10.1007/978-981-19-7618-6_9.

IRC SP-72. (1915). *Guidelines for the design of flexible pavements for low volumre rural roads.* IRC.

IRC SP-89. (2010). *Guidelines for soil and granular material stabilization using cement, lime & fly ash.* IRC.

IRC 37. (2018). *Guidelines for the design of flexible pavements.* IRC.

Ismail, I., Bernal, S.A., Provis, J.L., Nicolas, R.S., Hamdan, S.B., & Deventer, J.S.J. (2014). Modification of phase evolution in alkali-activated blast furnace slag by the incorporation of fly ash. *Cement and Concrete Composites*, 45, 125-135. https://doi.org/10.1016/j.cemconcomp.2013.09.006.

Jones, L.D., & Jefferson, I. (2023). Expansive soils. In M. Brown, J. Burland, T. Chapman, K. Higgins, H. Skinner & D. Toll (Eds.), *ICE manual of geotechnical engineering* (Vol. 1). Leeds: Emerald Publishing.

Kalipcilar, I., Mardani-Aghabaglou, A., Sezer, A., Altun, S., & Inan Sezer, G. (2018). Sustainability of cement-stabilised clay: sulfate resistance. *Proceedings of the Institution of Civil Engineers. Engineering Sustainability*, 171(5), 254-274. https://doi.org/10.1680/jensu.16.00005.

Kampala, A., & Horpibulsuk, S. (2013). Engineering properties of silty clay stabilized with calcium carbide residue. *Journal of Materials in Civil Engineering*, 25(5), 632-644. https://doi.org/10.1061/(ASCE)MT.1943-5533.0000618.

Kampala, A., Jitsangiam, P., Pimraksa, K., & Chindaprasirt, P. (2020). An investigation of sulfate effects on compaction characteristics and strength development of cement-treated sulfate bearing clay subgrade. *Road Materials and Pavement Design*, 22(10), 2396-2409. https://doi.org/10.1080/14680629.2020.1753564.

Kashani, A., Ngo, T.D., Walkley, B., & Mendis, P. (2017). Thermal performance of calcium-rich alkali-activated materials: a microstructural and mechanical study. *Construction & Building Materials*, 153, 225-237. https://doi.org/10.1016/j.conbuildmat.2017.07.119.

Khaksar Najafi, E., Jamshidi Chenari, R., Payan, M., & Arabani, M. (2021). A sustainable landfill liner material: clay-fly ash geopolymers. *Bulletin of Engineering Geology and the Environment*, 80(5), 4111-4124. https://doi.org/10.1007/s10064-021-02185-7.

Khater, H. (2014). Studying the effect of thermal and acid exposure on alkali-activated slag geopolymer. *Advances in Cement Research*, 26(1), 1-9. https://doi.org/10.1680/adcr.11.00052.

Kumar, S., Kumar, R., & Mehrotra, S.P. (2010). Influence of granulated blast furnace slag on the reaction, structure and properties of fly ash based geopolymer. *Journal of Materials Science*, 45(3), 607-615. https://doi.org/10.1007/s10853-009-3934-5.

Lee, W., & Van Deventer, J. (2002). The effects of inorganic salt contamination on the strength and durability of geopolymers. *Colloids and Surfaces. A, Physicochemical and Engineering Aspects*, 211(2-3), 115-126. https://doi.org/10.1016/S0927-7757(02)00239-X.

Lin, X., Zhang, D., Zhao, Z., Zhang, C., Ma, B., Zhou, H., Wang, Y., Xue, D., Tang, J., Chen, C., Li, J., Sun, Z., Zhang, H., & Li, W. (2024). High-performance geopolymers with municipal solid waste incineration fly ash: influence on the mechanical and environmental properties. *Buildings*, 14(11), 3518. https://doi.org/10.3390/buildings14113518.

Misra, A.K., Biswas, D., & Upadhyaya, S. (2005). Physico-mechanical behavior of self-cementing class C fly ash-clay mixtures. *Fuel*, 84(11), 1410-1422. https://doi.org/10.1016/j.fuel.2004.10.018.

Mistri, A., Bhattacharyya, S.K., Dhami, N., Mukherjee, A., & Barai, S.V. (2020). A review on different treatment methods for enhancing the properties of recycled aggregates for sustainable construction materials. *Construction & Building Materials*, 233, 117894. https://doi.org/10.1016/j.conbuildmat.2019.117894.

Mitchell, J.K. (1986). Practical problems from surprising soil behavior. *Journal of Geotechnical Engineering*, 112, 255-289. https://doi.org/10.1061/(ASCE)0733-9410(1986)112:3(255).

Mohammadinia, A., Arulrajah, A., Sanjayan, J.G., Disfani, M.M., Bo, M.W., & Darmawan, S. (2016). Stabilization of demolition materials for pavement base/subbase applications using fly ash and slag geopolymers: laboratory investigation. *Journal of Materials in Civil Engineering*, 28(7), 04016033. https://doi.org/10.1061/(ASCE)MT.1943-5533.0001526.

Nagajothi, S., & Elavenil, S. (2021). Effect of GGBS addition on reactivity and microstructure properties of ambient cured fly ash based geopolymer concrete. *Silicon*, 13(2), 507-516. https://doi.org/10.1007/s12633-020-00470-w.

Nanda, B., Mishra, J., & Patro, S.K. (2024). Synthesis of rice husk ash based alkaline activators for geopolymer binder systems: a review. *Journal of Building Engineering*, 91, 109694. https://doi.org/10.1016/j.jobe.2024.109694.

Nurlina, N., Alief, M.N., Rahmawati, Z., Nurherdiana, S.D., Susanto, T.E., & Fansuri, H. (2024). Compressive strength and water flux performance of type C and type F fly ash-based geopolymer membrane. *Archives of Metallurgy and Materials*, 69(3), 1107-1113. https://doi.org/10.24425/amm.2024.150931.

Palomo, A., Blanco-Varela, M.T., Granizo, M., Puertas, F., Vazquez, T., & Grutzeck, M. (1999). Chemical stability of cementitious materials based on metakaolin. *Cement and Concrete Research*, 29(7), 997-1004. https://doi.org/10.1016/S0008-8846(99)00074-5.

Palomo, A., Fernández-Jiménez, A., Kovalchuk, G., Ordoñez, L., & Naranjo, M. (2007). OPC-fly ash cementitious systems: study of gel binders produced during alkaline hydration. *Journal of Materials Science*, 42(9), 2958-2966. https://doi.org/10.1007/s10853-006-0585-7.

Panitsa, O.A., Kioupis, D., & Kakali, G. (2024). Advancing the sustainability of geopolymer technology through the development of rice husk ash based solid activators. *Sustainability*, 16(17), 7243. https://doi.org/10.3390/su16177243.

Part, W.K., Ramli, M., & Cheah, C.B. (2015). An overview on the influence of various factors on the properties of geopolymer concrete derived from industrial by-products. *Construction & Building Materials*, 77, 370-395. https://doi.org/10.1016/j.conbuildmat.2014.12.065.

Phetchuay, C., Horpibulsuk, S., Arulrajah, A., Suksiripattanapong, C., & Udomchai, A. (2016). Strength development in soft marine clay stabilized by fly ash and calcium carbide residue based geopolymer. *Applied Clay Science*, 127, 134-142. https://doi.org/10.1016/j.clay.2016.04.005.

Phummiphan, I., Horpibulsuk, S., Sukmak, P., Chinkulkijniwat, A., Arulrajah, A., & Shen, S. (2016). Stabilisation of marginal lateritic soil using high calcium fly ash-based geopolymer. *Road Materials and Pavement Design*, 17(4), 877-891. https://doi.org/10.1080/14680629.2015.1132632.

Phummiphan, I., Horpibulsuk, S., Phoo-ngernkham, T., Arulrajah, A., & Shen, S. (2017). Marginal lateritic soil stabilized with calcium carbide residue and fly ash geopolymers as a sustainable pavement base material. *Journal of Materials in Civil Engineering*, 29(2), 04016195. https://doi.org/10.1061/(ASCE)MT.1943-5533.0001708.

Porbaha, G. (1998). Ground improvement engineering – the state of the US practice: part 1. Methods. *Proceedings of the Institution of Civil Engineers - Ground Improvement*, 2(4), 189-190. https://doi.org/10.1680/gi.1998.020405.

Pourakbar, S., Asadi, A., Huat, B.B., & Fasihnikoutalab, M.H. (2015). Soil stabilisation with alkali-activated agro-waste. *Environmental Geotechnics*, 2(6), 359-370. https://doi.org/10.1680/envgeo.15.00009.

Puertas, F., Martínez-Ramírez, S., Alonso, S., & Vázquez, T. (2000). Alkali-activated fly ash/slag cements: strength behaviour and hydration products. *Cement and Concrete Research*, 30(10), 1625-1632. https://doi.org/10.1016/S0008-8846(00)00298-2.

Qian, Y., Yang, D., Zhao, J., Mao, X., Ren, G., & Cao, Z. (2025). Development of cementless alkali-activated ultra-high performance concrete under various steam curing regimes: mechanical properties, permeability, and microstructure. *Journal of Building Engineering*, 101, 111857. https://doi.org/10.1016/j.jobe.2025.111857.

Raja, K., Venkatachalam, S., Vishnuvardhan, K., Krishnan, R.S.R., Selvan, V.T., & Vetriselvan, N. (2022). A review on soil stabilization using rice husk ash and lime sludge. *Materials Today: Proceedings*, 65, 1205-1212. https://doi.org/10.1016/j.matpr.2022.04.178.

Ramon-Tarragona, A., & Alonso, E.E. (2020). Analysis of massive sulphate attack to cement-treated compacted soils. *E3S Web of Conferences*, 195, 01009.

Ranjbar, N., Kuenzel, C., Spangenberg, J., & Mehrali, M. (2020). Hardening evolution of geopolymers from setting to equilibrium: a review. *Cement and Concrete Composites*, 114, 103729. https://doi.org/10.1016/j.cemconcomp.2020.103729.

Riyap, H.I., Ngongang, B., Tchakouté, H.K., Nanseu-Njiki, C., & Rüscher, C. (2022). Compressive strengths and microstructural properties of geopolymeric materials arising from the addition of semi-crystalline alumina to silica-rich aluminosilicate sources. *Silicon*, 14(16), 10535-10558. https://doi.org/10.1007/s12633-022-01786-5.

Roskos, C., Cross, D., Berry, M., & Stephens, J. & Pe (2011). Identification and verification of self-cementing fly ash binders for " green " concrete. In *Proceedings of the 11th World Coal Ash (WOCA) Conference*, Denver, CO, USA.

Sahoo, N., Kumar, A., & Samsher. (2023). Potential of solar thermal calciner technology for cement production in India and consequent carbon mitigation. *Process Safety and Environmental Protection*, 179, 667-676. https://doi.org/10.1016/j.psep.2023.09.041.

Sakkas, K., Panias, D., Nomikos, P., & Sofianos, A. (2014). Potassium based geopolymer for passive fire protection of concrete tunnels linings. *Tunnelling and Underground Space Technology*, 43, 148-156. https://doi.org/10.1016/j.tust.2014.05.003.

Sarker, P.K., Kelly, S., & Yao, Z. (2014). Effect of fire exposure on cracking, spalling and residual strength of fly ash geopolymer concrete. *Materials & Design*, 63, 584-592. https://doi.org/10.1016/j.matdes.2014.06.059.

Scheuermann Filho, H.C., Miguel, G.D., & Consoli, N.C. (2022). Durability response of a cemented clayey sand over a wide range of porosities and cement contents. *Cleaner Materials*, 5, 100117. https://doi.org/10.1016/j.clema.2022.100117.

Scrivener, K.L., John, V.M., & Gartner, E.M. (2018). Eco-efficient cements: potential economically viable solutions for a low-CO_2 cement-based materials industry. *Cement and Concrete Research*, 114, 2-26. https://doi.org/10.1016/j.cemconres.2018.03.015.

Sepehrian, M., Yazdi, F., & Anbia, M. (2024). Extraction and green template-free synthesis of high-value mesoporous γ-Al_2O_3 and SiO_2 powders from coal gangue. *Powder Technology*, 444, 120023. https://doi.org/10.1016/j.powtec.2024.120023.

Sharma, L., Sirdesai, N., Sharma, K., & Singh, T. (2018). Experimental study to examine the independent roles of lime and cement on the stabilization of a mountain soil: a comparative study. *Applied Clay Science*, 152, 183-195. https://doi.org/10.1016/j.clay.2017.11.012.

Shehata, N., Mohamed, O., Sayed, E.T., Abdelkareem, M.A., & Olabi, A. (2022). Geopolymer concrete as green building materials: recent applications, sustainable development and circular economy potentials. *The Science of the Total Environment*, 836, 155577. https://doi.org/10.1016/j.scitotenv.2022.155577.

Silva, P., Sagoe-Crenstil, K., & Sirivivatnanon, V. (2007). Kinetics of geopolymerization: role of Al_2O_3 and SiO_2. *Cement and Concrete Research*, 37(4), 512-518. https://doi.org/10.1016/j.cemconres.2007.01.003.

Sim, S., Rhee, J.H., Oh, J.-E., & Kim, G. (2023). Enhancing the durability performance of thermally damaged concrete with ground-granulated blast furnace slag and fly ash. *Construction & Building Materials*, 407, 133538. https://doi.org/10.1016/j.conbuildmat.2023.133538.

Somna, K., Jaturapitakkul, C., Kajitvichyanukul, P., & Chindaprasirt, P. (2011). NaOH-activated ground fly ash geopolymer cured at ambient temperature. *Fuel*, 90(6), 2118-2124. https://doi.org/10.1016/j.fuel.2011.01.018.

Sun, Y., Yang, Y., Niu, X., Yang, J., Deng, K., Song, S., Shi, X., Wen, Z., & Wang, Y. (2024). Pavement performance of fine-grained soil stabilized by fly ash and granulated blast furnace slag-based geopolymer as road base course material. *Journal of Materials in Civil Engineering*, 36(7), 04024167. https://doi.org/10.1061/JMCEE7.MTENG-17236.

Suresh, R., & Murugaiyan, V. (2021). Influence of chemical admixtures on geotechnical properties of expansive soil. *International Journal of Engineering*, 34(1), 19-25.

Temuujin, J., van Riessen, A., & Williams, R.P. (2009). Influence of calcium compounds on the mechanical properties of fly ash geopolymer pastes. *Journal of Hazardous Materials*, 167(1-3), 82-88. https://doi.org/10.1016/j.jhazmat.2008.12.121.

Turner, L.K., & Collins, F.G. (2013). Carbon dioxide equivalent (CO_2-e) emissions: a comparison between geopolymer and OPC cement concrete. *Construction & Building Materials*, 43, 125-130. https://doi.org/10.1016/j.conbuildmat.2013.01.023.

Vafaei, M., Allahverdi, A., Dong, P., Bassim, N., & Mahinroosta, M. (2021). Resistance of red clay brick waste/phosphorus slag-based geopolymer mortar to acid solutions of mild concentration. *Journal of Building Engineering*, 34, 102066. https://doi.org/10.1016/j.jobe.2020.102066.

Wang, X., Wang, X., Lv, J., Yang, J., He, B., Han, P., & Bai, X. (2023). Mechanical properties and hydration behaviour of circulating fluidised bed fly ash- ground granulated blast furnace slag-lime ecofriendly cementitious material. *Construction & Building Materials*, 409, 133964. https://doi.org/10.1016/j.conbuildmat.2023.133964.

Wang, Q., Zhang, F., & Li, R. (2024a). Artificial intelligence and sustainable development during urbanization: perspectives on AI R&D innovation, AI infrastructure, and AI market advantage. *Sustainable Development (Bradford)*, 33(1), 1136-1156. https://doi.org/10.1002/sd.3150.

Wang, X., Liu, F., Pan, Z., Chen, W., Muhammad, F., Zhang, B., & Li, L. (2024b). Geopolymerization of coal gangue via alkali-activation: dependence of mechanical properties on alkali activators. *Buildings*, 14(3), 787. https://doi.org/10.3390/buildings14030787.

Wu, D., Zhang, Z., Chen, K., & Xia, L. (2022). Experimental investigation and mechanism of fly ash/slag-based geopolymer-stabilized soft soil. *Applied Sciences*, 12(15), 7438. https://doi.org/10.3390/app12157438.

Yan, S., Pan, D., Dan, J., Wang, J., & Yu, Y. (2023). Calcium carbide residue and Glauber's salt as composite activators for fly ash-based geopolymer. *Cement and Concrete Composites*, 140, 105081. https://doi.org/10.1016/j.cemconcomp.2023.105081.

Yi, Y.M., Zhu, D., Guo, S., Zhang, Z., & Shi, C. (2020). A review on the deterioration and approaches to enhance the durability of concrete in the marine environment. *Cement and Concrete Composites*, 113, 103695. https://doi.org/10.1016/j.cemconcomp.2020.103695.

Yusuf, M.O., Johari, M.A.M., Ahmad, Z.A., & Maslehuddin, M. (2014). Strength and microstructure of alkali-activated binary blended binder containing palm oil fuel ash and ground blast-furnace slag. *Construction & Building Materials*, 52, 504-510. https://doi.org/10.1016/j.conbuildmat.2013.11.012.

Zhang, M., Guo, H., El-Korchi, T., Zhang, G., & Tao, M. (2013). Experimental feasibility study of geopolymer as the next-generation soil stabilizer. *Construction & Building Materials*, 47, 1468-1478. https://doi.org/10.1016/j.conbuildmat.2013.06.017.

Zhang, A., Yang, W., Ge, Y., Du, Y., & Liu, P. (2021). Effects of nano-SiO2 and nano-Al_2O_3 on mechanical and durability properties of cement-based materials: a comparative study. *Journal of Building Engineering*, 34, 101936. https://doi.org/10.1016/j.jobe.2020.101936.

Zhang, B., Zhu, H., Feng, P., & Zhang, P. (2022). A review on shrinkage-reducing methods and mechanisms of alkali-activated/geopolymer systems: effects of chemical additives. *Journal of Building Engineering*, 49, 104056. https://doi.org/10.1016/j.jobe.2022.104056.

Zinchenko, A., Sakai, T., Morikawa, K., & Nakano, M. (2022). Efficient stabilization of soil, sand, and clay by a polymer network of biomass-derived chitosan and carboxymethyl cellulose. *Journal of Environmental Chemical Engineering*, 10(1), 107084. https://doi.org/10.1016/j.jece.2021.107084.